Estimating the spatial variability of water consumption in the Karkheh river basin, Iran - using MODIS data

Lal P. Muthuwatta, Mobin-ud-Din Ahmad, Tom H.M. Rientjes and Marinus G. Bos

Abstract: Spatially distributed actual evapotranspiration (ET_a) values were estimated based on satellite data and the Surface Energy Balance System (SEBS) approach for the Karkheh River Basin, Iran. Nineteen cloud free MODIS (Moderate Resolution Imaging Spectroradiometer) images, representing a complete cropping year from November 2002 to October 2003 were acquired and processed. Estimated ET_a values were verified using sub-catchment scale water balance analysis. The results revealed that during the study period ET_a was estimated at 16680x10^6m^3 and that the water balance closure terms at sub-basin scale ranged from 0.6% to 7.2% of precipitation. This implies that water balance is sufficiently understood. Estimated outflow from the basin was 7.8% of precipitation and indicates that water is a very scarce resource in the Karkheh. Rain fed areas consume about 3720 x10^6 m^3/year and are mainly located in the sub-catchments of the upper Karkheh while irrigated areas consume 2680x 10^6 m^3/year and are mainly located in the lower areas in the basin. Total water consumption by forest is about 2070×10^6 m^3/year, mainly in the middle parts of the basin. The range lands are scattered mainly all over the Upper Karkheh and together with areas in the Lower Karkheh consume about 3360×10^6 m^3/year. ET_a from other land uses is 4110×10^6 m^3/year, of which ET_a from open water surfaces is the main contributor. The Karkheh Dam evaporates 80×10^6 m^3/year while wetlands located in the lower area of the basin evaporate 660×10^6 m^3/year. Satellite data along with the SEBS algorithm and geo-statistical techniques are effective to estimate spatial patterns of water consumption and availability. These facilitate the introduction of diverse management interventions to different areas in the basin based on the real ground situation.

Keywords: actual evapotranspiration, SEBS, MODIS, water balance, Karkheh river basin

Lal P. MUTHUWATTA
International Water Management Institute,
P.O. Box 2075, Colombo, Sri Lanka
Tel: +94-112880000
Fax: +94-112786854
l.mutuwatte@cgiar.org

Mobin-ud-Din AHMAD
CSIRO, Land and Water
GPO Box 16666, Canberra
ACT2601 - Australia
Mobin.Ahmad@csiro.au

Tom H.M. RIENTJES
Water Resources Department,
Faculty of Geo-Information Science and Earth Observation,
University of Twente
PO Box 6, 7500 AA Enschede
The Netherlands
rientjes@itc.nl

Marinus G. BOS
Bos-Water
Generaal Foulkesweg 68F
6703 BW Wageningen
The Netherlands
marinusgbos@cs.com

Received: 27 august 2010 / Accepted: 1 december 2010
Published online: 31 december 2010

Riassunto: *La distribuzione spaziale dei valori dell'evapostraspirazione reale (ET_a) è stata stimata basandosi su dati da satellite e attraverso l'utilizzo del metodo di Surface Energy Balance System (SEBS) nell'area del Bacino Idrografico del Fiume Karkheh, in Iran.*

Sono state acquisite e processate novantanove immagini MODIS (Moderate Resolution Imaging Spectroradiometer) libere da nubi, che rappresentano la completa copertura di un anno dal novembre 2002 all'Ottobre 2003. I valori di ET_a stimati sono stati verificati attraverso l'analisi del bilancio idrico alla scala di sottobacino.

I risultati hanno rilevato che durante il periodo di studio ET_a è stato stimato in 16680x10^6 m^3 e che i termini finali del bilancio idrico alla scala di un sottobacino variavano da 0.6% al 7.2% delle precipitazioni. Da tali risultati è stato ritenuto che il bilancio idrico sufficientemente valido. Il deflusso stimato dal bacino era circa 7.8% delle precipitazioni e indica che l'acqua è una risorsa molto scarsa nel Karkheh. Le aree alimentate dalla pioggia consumano circa 3720x10^6 m^3/anno e si trovano soprattutto nel sub-bacini della Karkheh superiore, mentre le aree irrigate consumano 2680x 10^6 m^3/anno e si trovano principalmente nelle zone più basse del bacino. Il consumo totale di acqua da parte della zona boschiva è di circa 2.070× 10^6 m^3/anno, ed è localizzata soprattutto nella parte centrale del bacino. L'estensione delle aree a pascolo è distribuita in gran parte nel Karkheh superiore e insieme con le aree della Bassa Karkheh consumano circa 3.360×10^6 m^3/anno. ET_a per altri usi del suolo è 4.110×10^6 m^3/anno, di cui l'ET_a dalle acque superficiali genera il principale contributo. La diga di Karkheh evapora 80×10^6 m^3/anno, mentre le zone umide che si trovano nella zona bassa del bacino evaporano 660×106 m^3/anno. I dati satellitari applicati insieme con l'algoritmo SEBS e tecniche di elaborazione geo-statistica sono efficaci per valutare i modelli spaziali del consumo dell'acqua e della sua disponibilità. Tali tecniche facilitano l'introduzione di numerosi interventi di gestione per le diverse aree del bacino sulla base della situazione reale sul terreno.

Introduction

Information on the spatial distribution of actual evapotranspiration (ET_a) is crucial for water management in river basins. Especially in water scares river basins where there is increasing pressure on water resources, a sound knowledge is required on how water is used in order to make better allocation decisions. For example, linking crop yields with related ET_a can be used to estimate the productivity

 DOI 10.4409/Am-016-10-0015

of water. Some areas produce higher crop yields while some other areas produce lower crop yields by consuming the same amount of water. Information on such variations in productivity is important to plan strategies to reallocate water in order to improve productivity (e.g. Teixeira et al., 2008).

Often there is a lack of field data on the actual consumption of water and this hampers judicious management and planning of water resources. In many water resources studies it is practice that ET_a is estimated as a residual to close the water balance. For instance, Domingo et al. (2001) and Loukas et al. (2005) calibrated a catchment scale stream flow model by changing ET_a. In these studies, estimations of ET_a cannot be considered reliable since estimated ET_a obscures and compensates for any shortcomings and limitations of the modeling approach (Muthuwatta et al, 2010). Another procedure to estimate field specific ET_a is through reference evapotranspiration (ET_0) and crop coefficients (K_c) that correct for water stress. In this procedure measurements from meteorological stations are used to estimate ET_0 for reference grass. The estimation of ET_a for different crops is carried out by multiplying ET_0 with respective crop coefficients and water stress coefficients (K_s) (see Allen et al., 1998; Bos et al., 2009). More advanced field procedures to estimate ET_a are based on eddy correlation techniques and scintillometer data (see Hemakumara et al., 2003). However, a limitation of these approaches is that the information is obtained only for small areas and estimates of ET_a over larger areas are not ascertained. In this respect, considering effects of spatial and temporal variations of surface characteristics on ET_a cannot be assured (see Ahmad et al., 2006).

The development of remote sensing (RS) sensors and techniques during the last few decades triggered the development of methods to estimate spatially distributed ET_a over large areas. These methods are based on the energy balance approach (Bastiaanssen et. al., 1998, Su, 2002) and these models have been used to create a variety of applications in many river basins in the world (Ahmad, 2005; Bastiaanssen and Chandrapala, 2003; Mutuwatta et al., 2010). Among the several ET_a estimation methods, remote sensing methods are regarded as the only technology that can efficiently and economically provide regional and global coverage of actual water consumption by different land cover classes on the ground (Tasumi, 2003). In addition, satellite observations can be repeated over time. These two features allow aggregation of hydrological indicators over large spatial domains for selected time periods. At the same time, freely available satellite images from the internet make the applications of these methods cost effective. This paper presents the application of the Surface Energy Balance Systems (SEBS), using freely available Moderate Resolution Imaging Spectroradiometer (MODIS) images, to compute actual evapotranspiration in the Karkheh River Basin, Iran. This is the first attempt to estimate evapotranspiration using satellite image in the basin.

Study area

The Karkheh River Basin (51,000 km^2) is located in the south-western region of Iran. between 30° to 35° northern latitude and 46° to 49° eastern longitude (Fig. 1). It is one of the most productive river basins in Iran and occupies 9% of the total irrigated area of the country. Also some 10-11% of the country's wheat production comes from the basin (Marjanizadeh, 2008). Water in the basin is mainly used for agriculture production, domestic supplies, and fish farming but also serves to sustain the environment. For the latter, a major concern is the sustainability of the Hoor-Al-Azim swamp, a Ramsar site located at the Iran-Iraq border. Hydrologically the basin is di-

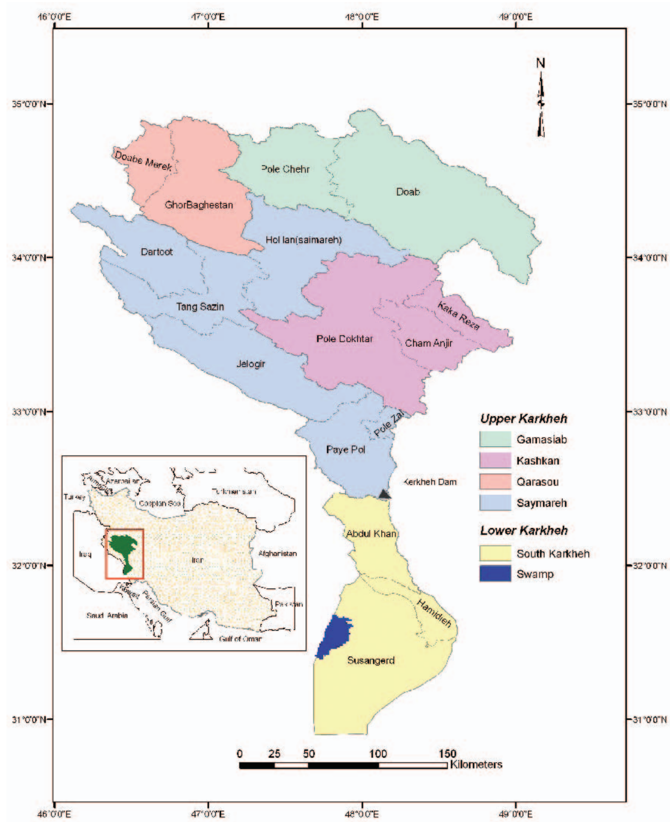

Fig. 1: *Location of the Karkheh river basin and sub-basins.*

vided into five sub-basins, Gamasiab, Qarasou, Kashkan, Saymareh and south Karkheh (Fig. 1). The first four sub-basins are major tributaries to the main stream of the Karkheh River while Lower Karkheh or South Karkheh is the area south of the Karkheh dam.

The elevation of the basin ranges from less than 10 m above mean sea level in the south to more than 3500 m in the north of the basin. The southern part of the basin receives annual average precipitation of about 150 mm while in the northern part it can reach up to 750 mm. In the Lower and Upper Karkheh, maximum summer temperature goes up to 45°C and 35°C respectively. Class A pan evaporation, which is the sole readily available evaporation data in the basin, ranges from 2000-3600 mm from the North to the South. Precipitation in the Lower Karkheh area is regarded as insufficient to meet crop water requirements and irrigated agriculture largely depends on water from the Karkheh dam and from groundwater resources. Rangelands, rainfed agriculture, forests and irrigated agriculture are the main land uses in the basin. In the upper basin areas both rainfed and irrigated agriculture are practiced while only irrigated agriculture is practiced in the arid climate lower basin. The Karkheh reservoir has a storage capacity of 7500x10^6 m^3 with a live storage capacity of about 4700x10^6 m^3 and has been operational since 2002. The reservoir is designed to irrigate 320,000 ha of agricultural land in the Lower Karkheh. During November 2002 to October 2003 the accumulated dam outflow was measured at 2851x10^6 m^3. The growing competition between the various uses of water is among the major concerns in the basin. In the lower basin, the competition between irrigated agriculture and the wetland ecosystem has led to low water productivity, increasing salinity problems and reduced surface water availability. Under these circumstances, knowledge on spatial and temporal patterns of water consumption is vital for planners and water managers.

Methodology and data

Surface energy balance algorithm.

In this study the Surface Energy Balance System (SEBS) proposed by Su (2002) was used. SEBS has been developed to solve surface energy balance by integrating remote sensing data with in-situ meteorological data. The surface energy balance is given by:

$$R_n = G_0 + H + \lambda E \tag{1}$$

Where Rn is the net radiation (Wm^{-2}), G_0 is the soil heat flux (Wm^{-2}), H is the sensible flux (Wm^{-2}) and λE is the latent heat flux (Wm^{-2}) associated with the transfer of moisture into the atmosphere.

The land surface parameters (surface albedo, emissivity, surface temperature, fractional vegetation cover and leaf area index) for the system are extracted from the reflectance and radiance measurements of the satellite. The other inputs include air pressure, temperature, humidity, and wind speed. The third input are the radiation components derived through parameterization (see, Su, 2002). To determine the evaporative fraction, SEBS uses the energy balance consideration at limiting cases proposed by Menenti and Choudhury (1993). At dry limit, the whole area is assumed as dry. The latent heat (or the evaporation) then becomes zero due to the limitation of soil moisture and the sensible heat flux is at its maximum value. Equation (1) then becomes:

$$H_{dry} = R_n - G_0 \tag{2}$$

Under the wet limit, the whole area is assumed to be wet and evaporation takes place at its potential rate. At this limit it is reasonable to assume that the sensible heat flux takes its minimum value. Therefore equation (1) could be rewritten as follows.

$$H_{w} = R_n - G_0 - \lambda E_{wet} \tag{3}$$

The relative evaporation is defined as:

$$\Lambda_r = \frac{\lambda E}{\lambda E_{wet}} = 1 - \left[\frac{H - H_{wet}}{H_{dry} - H_{wet}} \right] \tag{4}$$

The evaporative fraction is computed by the following relationship:

$$\Lambda = \frac{\lambda E}{R_n - G_0} = \frac{\Lambda_r . \lambda E_{wet}}{R_n - G_0} \tag{5}$$

The net available energy ($R_n - G_0$) in the above equation may have different time scales. For a time scale of one day or longer, G_0 can be ignored and the net available energy reduced to net radiation (R_n) (Bastiaanssen et. al., 1998).

By assuming that the daily value of the evaporative fraction is approximately equal to the instantaneous value, the daily evapotranspiration is determined as:

$$ET_{24} = \frac{8.64.10^7}{\lambda \rho_w} \Lambda . R_{n24} \quad \text{(mm/day)} \tag{6}$$

where R_{n24} (Wm^{-2}) is the 24 hour averaged net radiation, λ ($J\,Kg^{-1}$) is the latent heat of vaporization, and ρ_w ($Kg\,m^{-3}$) is the density of water.

This algorithm has been used on a variety of applications, including evaporation estimates in the Taiyuan Basin in China (Jin et al., 2005), Spain Barrax (Su and Jacobs, 2001), estimation of sensible heat flux in the Spanish Tomelloso area (Jia et al., 2003), and for drought monitoring purposes in North West China (Su et al., 2003).

Data used

Meteorological and river discharge data for the study period November 2002 to October 2003 have been collected from organizations and authorities that are responsible for its monitoring (Tab. 1). Daily stream flow data is collected at 4 gauging stations to estimate the out flow from the major sub-basins in the Upper Karkheh, . Inflow and outflow volumes of the Karkheh dam were only available from July 2002 onwards. Using the locations of river gauging stations and a Shuttle Radar Topography Mission (SRTM) digital elevation model (acquired from http://srtm.csi.cgiar.org/), the upstream contributing area for each river gauging station was estimated.

Table 1: *Meteorological and stream flow data available for Karkheh*

Parameter	Frequency	Source
Maximum and Minimum Air Temperature (Celsius)	Daily	Islamic Republic of Iran meteorological organization (IRIMO)
Relative Humidity (%)	three hourly	IRIMO
Wind speed (m/s)	three hourly	IRIMO
Sunshine hours (hours)	daily	IRIMO
Precipitation (mm)	daily	IRIMO
Stream flow (m^3/day)	daily	Iranian Power Ministry

For estimation of ET_a, 19 cloud free MODIS-TERRA images covering the study area were acquired for the period November 2002 to October 2003 (Tab. 2). Land use was classified using the time series of MODIS-TERRA with bands in the visible, near infrared and thermal infrared areas of the electro magnetic spectrum.

Table 2: *Acquisition dates of TERRA-MODIS images from November 2002 to October 2003. (Source: http://ladsweb.nascom.nasa.gov/)*

Year	Jan	Feb	Mar	Apr	May	Jun
2002						
2003	12	06	15	29	24	05,19
Year	**Jul**	**Aug**	**Sep**	**Oct**	**Nov**	**Dec**
2002					03	08
2003	02	02,10,22	07,16,25	06,11,25		

Processing of MODIS data

In order to use MODIS data as an input for SEBS, different processing steps have to be followed. For this, Integrated Land and Water Information System (ILWIS) image processing software developed by ITC, The Netherlands is used. The energy balance algorithm used in this study needs broad band surface albedo, emissivity, surface temperature, fractional vegetation cover and leaf area index from satellite data.

 DOI 10.4409/Am-016-10-0015

Broadband surface albedo, ρ_{sw}, has been calculated from Surface Reflectance using the empirical relation of Liang (2000):

$$\rho_{sw} = 0.160\times\alpha_1 + 0.291\times\alpha_2 + 0.243\times\alpha_3 + 0.116\times\alpha_4 + 0.112\times\alpha_5 + 0.081\times\alpha_7 - 0.0015 \quad (7)$$

where α_n is the reflectance of band n. This estimated ρ_{sw} is used to calculate net incoming radiation given in equation 8.

$$R_n = (1 - r_0)\cdot K^{\downarrow} + \varepsilon_s \cdot \varepsilon_a \cdot \sigma \cdot T_a^{\,4} - \varepsilon_s \cdot \sigma \cdot T_s^{\,4} \quad (8)$$

where r_0 = the broad band surface albedo (-), $K^{\downarrow}$ = the downward solar radiation (Wm^{-2}), ε_a = the emissivity of air (-), ε_s = the surface emissivity (-), σ = the Stefan-Boltzmann constant (Wm^{-2}K^{-4}), T_a = the air temperature (K) and T_s = the surface temperature (K) measured by a remote sensor.

The surface emissivity has being estimated using following equation proposed by Valor and Caselles (1996):

$$\varepsilon_s = 0.985\times f_c + 0.96\times(1-f_c) + 4\times 0.015\times f_c\times(1-f_c) \quad (9)$$

where f_c is the fractional vegetation cover.

The fractional vegetation cover (f_c) is derived from NDVI, using the following equation (Choudhury et al.,1994):

$$f_c = 1 - \left(\frac{NDVI_{\max} - NDVI}{NDVI_{\max} - NDVI_{\min}}\right)^{0.625} \quad (10)$$

where NDVImin is the NDVI for bare soil and NDVImax is the NDVI for full vegetation cover.

Land surface temperature was calculated based on the brightness temperature estimated using MODIS bands 31 and 32 and the method proposed by Kerr et al. (1992).

Results

Daily ET_a maps were estimated by applying the SEBS algorithm to 19 cloud free MODIS images. Incorporating evaporative fraction maps and average net daily radiation maps with the equation 6, monthly and annual ET_a maps were prepared. Figure 2 shows the spatial distribution of annual ET_a from November 2002 to October 2003.

The annual ET_a, for the period November 2002 to October 2003 ranges from 40 mm to 1680 mm. The highest value is found in the Karkheh reservoir and the lowest in the bare land/desert areas downstream of the Karkheh dam. Cropped areas show large spatial variations in the annual ET_a. For example, the ET_a values associated with the rainfed areas are 396 mm/year and 714 mm/year for irrigated crops. However, there are large variations found within the same land use. In the map, irrigated areas in the upper and lower Karkheh are shown by high ET_a values. The large red area in the lower part of the basin shows the low ET_a in the desert while the large blue patch in the Lower Karkheh indicates the higher ET_a in the Hoor-Al-Azim swamp. To quantify the water consumption by major land uses in the KRB, ET_a and classified land use maps based on the time series of MODIS satellite data (Ahmad et al., 2009) are used. Figure 3 presents the annual ET_a volumes by major landuse classes in KRB between November 2002 and October 2003.

In KRB irrigated agricultural areas cover about 509700 ha and there about 1389000 ha under rainfed agriculture, this is the reason for the higher total volume of ET_a for the rainfed agriculture areas. Further analysis revealed that ET_a in different land use classes show large ranges between maximum and minimum values. For instance, some irrigated areas consume less than 300 mm/year of water while

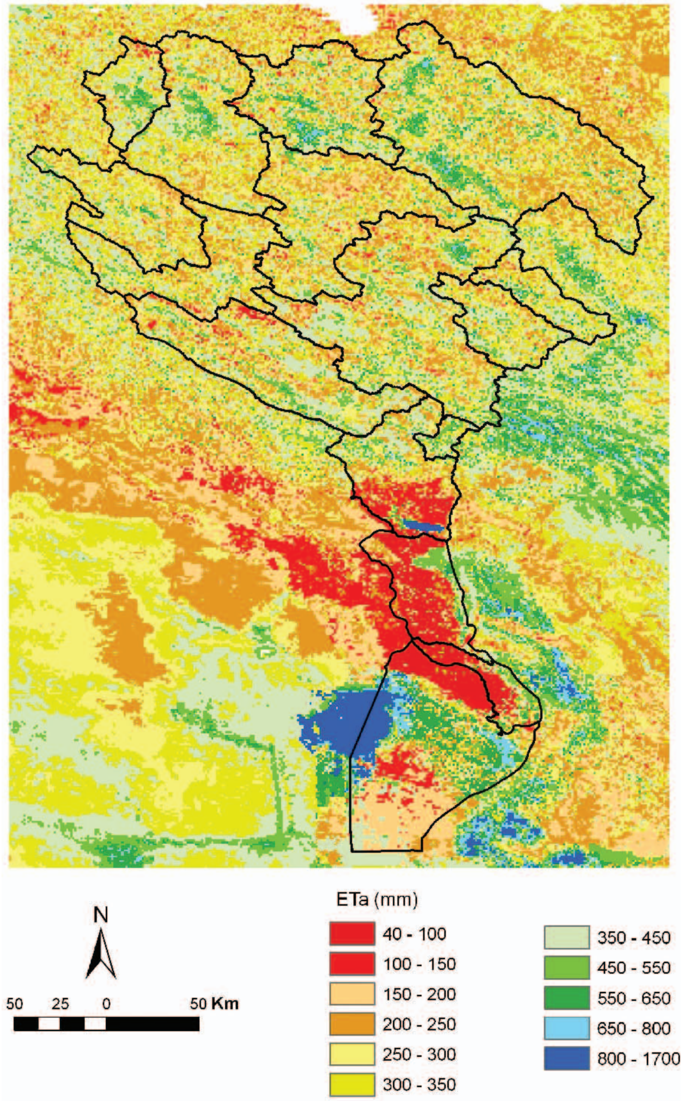

Fig. 2: *Annual actual evapotranspiration (ET_a) in the Karkheh Basin - November 2002 – October 2003.*

some other areas consumes closer to 700 mm/year. Average ET_a is highest for the irrigated areas while the lowest values are found in bare land areas. Average ET_a per unit land area in rainfed agricultural is significantly lower than that in irrigated areas. This is evident by the yields, as in wheat areas average irrigated yield is about two fold higher than the average yield in rainfed areas (Ahmad et al., 2009). Average ET_a associated with the rangelands is 316 mm/year and the maximum value is more than 500 mm/year. This shows some possibilities to expand rainfed agricultural areas into rangelands areas whenever other conditions such as land slope and accessibility is suitable. In that sense, less beneficial ET_a from the range lands can be used to produce more crop yield. In this way total production can be improved without developing new water resources. This is very important for Karkheh River Basin as the basin already experiences water scarce conditions while the demand for food are rising due to the increasing population.

Further, the quantitative information on ET_a is important to identify the areas where water stress limits the crop production and also the crop areas that consume more water than the recommended values. Figure 4 presents the spatial variation of ET_a in the Gamasiab

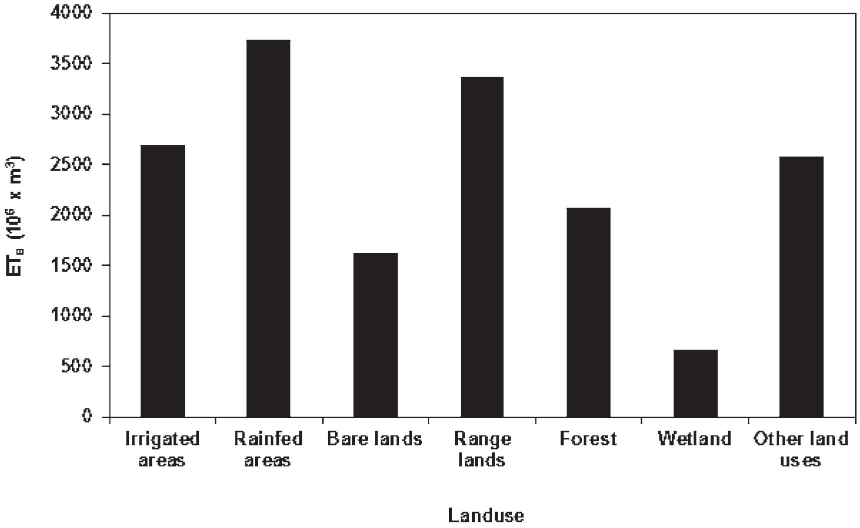

Fig. 3: *Annual ET_a for different land use classes in the Karkheh River Basin.*

sub-basin in upper Karkheh. In Figure 5, the areas under different ET_a intervals are presented.

Land use classes in the Gamasiab sub-basin include irrigated agricultural lands, rain fed agricultural lands, forest areas, orchards and bare lands. Figure 4 shows the 1 km^2 pixel scale distribution of ET_a over the sub-basin and is ranging from less than 200 mm/year to more than 600 mm/year. Comparing the ET_a map with the landuse map of the sub-basin reveal that high values of ET_a are found in the irrigated areas and low values are from bare land areas. In most of the rainfed agricultural areas in the sub-basin the ET_a is between 200 to 350 mm/year. The ET_a map (Fig. 4) is classified into different intervals and the land area under each ET_a interval is estimated (Fig. 5). ET_a associated with the majority of the areas is between 200 and 400 mm/year. Further, using the landuse map, the ET_a was extracted for irrigated wheat areas. Wheat season in the Upper Karkheh is from November to July. Wheat areas under different seasonal ET_a intervals and the associated yield values are presented in Figure. 6. To estimate the average wheat yields in different ET_a intervals, data (Ahmad et al., 2009) from a field survey (Ahmad et al., 2009) is used.

As shown in Figure 6, about 70% of the areas are in the ET_a interval of 250 to 450 mm/season. Highest reported yield is 5800 kg/ha and is found in the ET_a interval 350 to 400 mm/season. Thereafter, the yield values fluctuate closer to 5800 kg/ ha. Therefore, the optimum ET_a interval for the highest wheat yield could be considered as 350 to 400 mm/season. This indicates that there are about 29100 ha of wheat area consuming water less than what is sufficient to maximize the yield, while another 26600 ha of wheat lands consume more water than the sufficient amount. This indicates that by reallocating water from high ET_a areas to low ET_a areas wheat production can be improved.

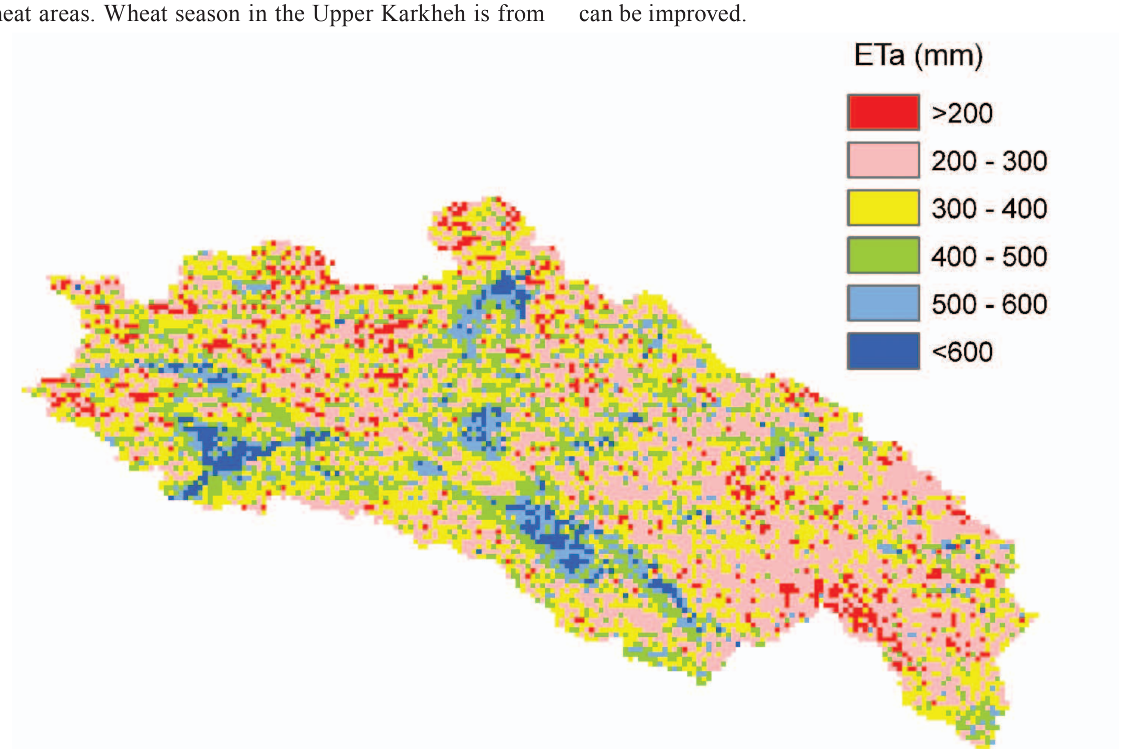

Fig. 4: *Spatial variation of ET_a in Gamasiab sub-basin.*

DOI 10.4409/Am-016-10-0015

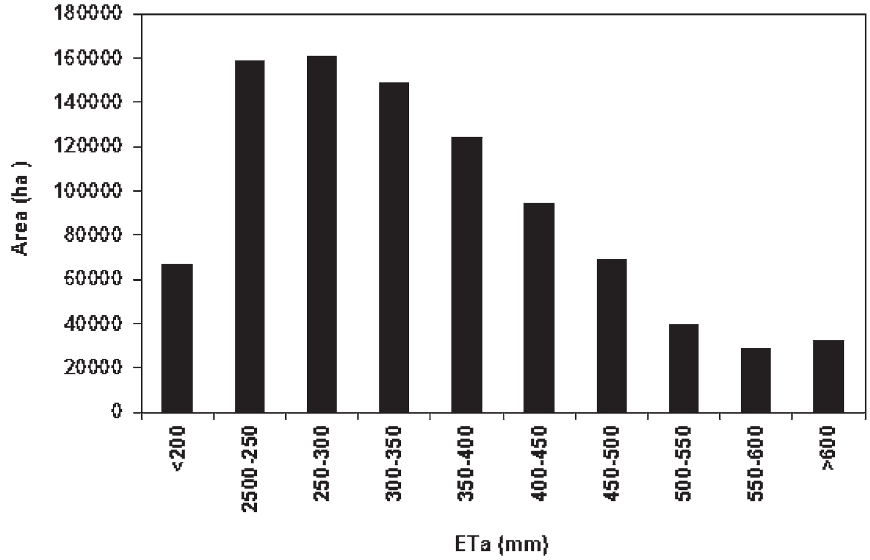

Fig. 5: *Areas under different ET_a intervals.*

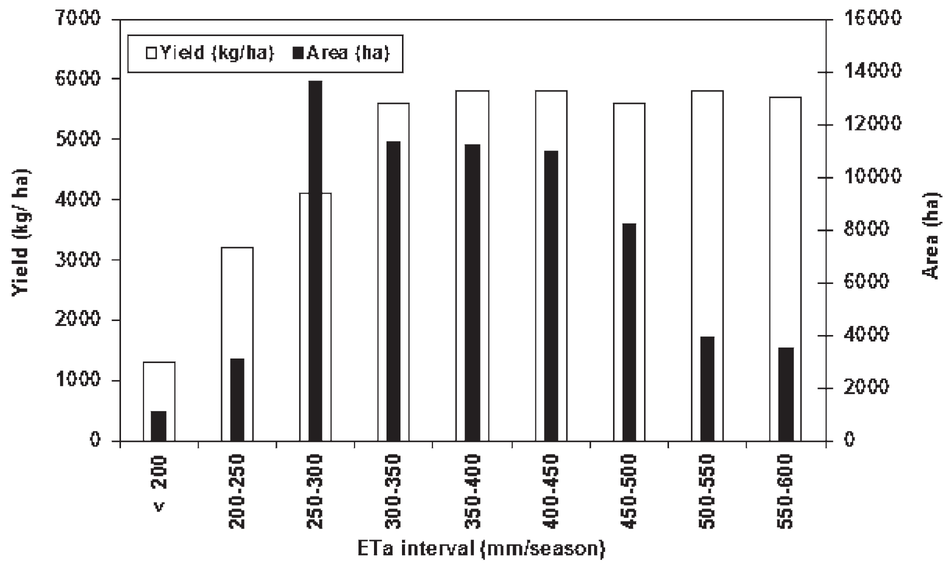

Fig. 6: *Land areas under different ET_a intervals and related yields in wheat areas in the Gamasiab sub-basin.*

Water Balance

The sub-basin scale annual water balance is computed using Equation 11 and values are presented in Tab. 3. Interpolated precipitation data (Muthuwatta et al., 2010), satellite based ET_a and observed stream flow data were used. For each sub-basin mean values of ET_a and precipitation are defined by dividing the sum of pixel values by the number of pixels. These values were converted into volume by multiplication with sub-basin areas to allow volumetric assessments.

$$P + Q_{in} + G_{in} - ET_a - Q_{out} - G_{out} = \Delta S \qquad (11)$$

where P is the precipitation, Q_{in} is the surface water inflow, G_{in} is the groundwater inflow, ET_a is the actual evapotranspiration, Q_{out} is the surface water outflow, G_{out} is the groundwater outflow, and ΔS is the storage change in ground water, surface water and soil water during the time interval considered. It is assumed that change in groundwater storage can be negligible as the water balance is solved for a full hydrological year.

During the cropping year November 2002 and October 2003 precipitation was 18507x10^6 m^3 while ET_a was 16680x10^6 m^3 water volume increase in the Karkheh reservoir during the same period was 368x10^6 m^3. Annual water balance was estimated for the whole KRB based on precipitation, ET_a and the volume change in the reservoir by assuming that during one cropping year storage changes in groundwater is negligible. The residual term of the water balance was 1459x10^6 m^3, which is 7.8% of the precipitation. For the Upper Karkheh (the area above the Karkheh dam) the water balance residual term was 2.9% relative to the annual precipitation in that area. Further, the sub-basin scale water balance residual terms ranged from 0.6% to 7.2% of the precipitation. This implies that water balance is sufficiently understood and it indirectly validates the ET_a.

Table 3: *Water balance for the whole basin and major sub–basins (m^3x10^6) from November 2002 to October 2003 (Source: Muthuwatta et al, 2010).*

Sub-basin	***Precipitation*** *(P)*	***Surface inflow*** (Q_{in})	***Actual evapotranspiration*** (ET_a)	***Surface/Reservoir change in storage*** (ΔS_S)	***Surface outflow*** (Q_{out})	***Closure %***
Gamasiab	4784	-	3697	-	742	7.2
Qarasou	2230	-	1764	-	399	3.0
Kashkan	4108	-	3143	-	939	0.6
Saymareh	6437	2079	5223	368	2851	1.1
Upper Karkheh	17559	-	13827	368	2851	2.9
Lower Karkheh	948	2880	2853	-	Not available	
Whole basin	18507	-	16680	368	Not available	

Discussion

ET_a estimation by SEBS uses some relationships based on simplified assumptions to estimate energy fluxes. These formulations use some empirical constants that could introduce some error to the estimation of ET_a. In this study, emissivity of the air, incoming long wave radiation and the temperature at the planetary boundary layer were estimated as a function of air temperature. For this, maps of air temperature were constructed based on interpolation by use of recorded data at the meteorological stations. Again, we speculate that this could introduce some errors to the abovementioned quantities and to the final ET_a estimation. In this study aerodynamic roughness height values were defined for separate land use classes. Since values are somewhat arbitrarily defined this causes uncertainty that becomes more pronounced when considering the large number of mixed pixels.

To estimate monthly and annual ET_a the evaporative fractions estimated in the days satellite data were available were considered as representative for specified time intervals (Equation 6). These intervals were selected in such a way that the date of the selected image is in the middle or close to the middle of the interval. Bastiaanssen et al. (2002) used this method to estimate time integrated ET_a by a set of NOAA-AVHRR images and validated the procedure by a set of ET_a values as estimated by the Bowen ratio method. In that study the time between consecutive cloud free images ranged between 2 and 35 days. In the present study, only two time intervals that are 37 and 45 days are outside that range. These intervals were found in February and April and fall in the rainy season. Farah et al. (2004) stated that the soil moisture dynamics and, thus, indirectly the rainfall events, control the long term seasonal variations of evaporative fraction. Therefore, we hypothesize that the assumption of the representative evaporative fraction over those two intervals can be justified since significant changes in soil moisture are not to be expected during the rainy season.

Conclusion

MODIS images along with the SEBS approach make it possible to estimate spatial distribution of actual evapotranspiration over the KRB. Total water evaporated from the basin during the one year study period was 16680 x 10^6 m^3. Estimating water consumed by different land use classes gives better insight to water managers and planners about how water is consumed. This information is vital to make water allocation decisions among different stakeholders, including the Hawr-Al-Azim swamp, a Ramsar site. In addition, information on water use by different land use classes could be useful to carry out basin and sub-catchment scale water accounting that requires depleted water in different categories. Satellite data along with the SEBS algorithm are usefulo to estimate spatial patterns of water consumption. In addition the pixel based spatially distributed information derived in this study could be used to identify the areas that receive less water. These facilitate the introduction of different management interventions to different areas in the basin based on the real ground situation.

For the Upper Karkheh the residual term in the water balance is 2.9% when normalized to the precipitation. Since there are no measured discharges of inflow in the swamp, closure of the water balance could not be established for the Lower Karkheh and thus for the entire basin. For the whole basin, however, the difference between precipitation and ET_a was 1825x10^6 m^3 while the water storage increase in the reservoir was 368x10^6 m^3 for the period of the study. Therefore, the unaccountable volume of water was 1457x10^6 m^3, 7.8% of the precipitation. This is the maximum possible outflow from the basin for the study period but presumably the outflow will be lower since recharge to the ground water system occurs. This implies that the basin is a very water scarce basin. In this respect it must be noted that it is important to maintain the flow into the swamp to guarantee sustainability of the wetland ecosystem.

Therefore we conclude that for the Karkheh basin the most viable option to increase agricultural production is to improve water productivity rather than to focus on the development of additional water resources. Information on the relationship between ET_a and the related crop yields (presented in Fig. 6) are especially important as it shows the areas that consumes more than sufficient water. Reallocating the surplus water from these areas to water deficit areas it is possible to maximize the production by same available water resources. This strategy will be a useful one in a basin such as Karkheh where opertunities to develop additional water resources are slim.

A satellite based energy balance approach and geo-statistical techniques have shown to be effective in estimating spatial patterns of water consumption. We hypothesize that spatially distributed information produced in this study could be used in various applications in the field of water management. For example (1) spatial patterns of ET_a over the irrigated areas could be used to identify the areas that

 DOI 10.4409/Am-016-10-0015

receive too little water; (2) information on water use by different land uses could serve to assess effects of land use changes on hydrology; and (3) ET_a as an indicator of water consumption for various crops could be used to assess water productivity in agricultural areas. Furthermore, results from this study facilitate the introduction of management interventions to different areas in the basin based on the actual catchment conditions.

Acknowledgment: The authors would like to acknowledge the valuable help provided by the Karkheh Basin Focal Project team members, especially Mr. Ilyas Masih, Dr. Hugh Turral and Mr. Poolad Karimi. Special thanks to the Iranian Meteorological Organization and the Energy Ministry of Iran for providing data for the study. This study was jointly financed by the International Water Management Institute (IWMI), the International Institute for Geo-Information Science and Earth Observation (ITC) and the Challenge Program of Water and Food (CPWF) for which their donors are acknowledged.

References

Ahmad M.D., Islam A., Mashi I., Muthuwatta L.P., Karimi P., Turral H.M. (2009) - Mapping basin-level water productivity using remote sensing and secondary data in the Karkheh River Basin, Iran. Water International, 34:1,119-133. DOI: 10.1080/02508060802663903

Ahmad M.D, Bastiaanssen W.G.M., Feddes R.A. (2005) - A new technique to estimate net groundwater use across large Irrigated areas by combining remote sensing and water balance approaches, Rechna Doab, Pakistan. Hydrogeolog Journal 13: 653-664. DOI: 10.1007/s10040-004-0394-5

Ahmad M.D., Biggs T., Turral H., Scott C.A. (2006) - Application of SEBAL approach and MODIS time-series to map vegetation water use patterns in the data scarce Krishna river basin of India IWA J. Water Science and Technology 53(10): 83-90. DOI: 10.2166/wst.2006.301

Allen R.G., Pereira L.S., Raes D., Smith M. (1998) - Crop evapotranspiration : guidelines for computing crop water requirements. FAO irrigation and drainage paper, 56. FAO, 300 pp.

Bastiaanssen W.G.M., Chandrapala L. (2003) - Water balance variability across Sri Lanka for assessing agricultural and environmental water use. Agricultural water management, 58(2):171-192. DOI:10.1016/S0378-3774(02)00128-2

Bastiaanssen W.G.M., Ahmad M.D., Chemin Y. (2002) - Satellite surveillance of evaporative depletion across thr Indus Basin. Water resource research, 38, 12,01273. DOI:10.1029/2001WR000386

Bastiaanssen W.G.M., Menenti M, Feddes R.A., Holtslag A.A.M. (1998). - A remote sensing surface energy balance algorithm for land (SEBAL):1. Formulation. Journal of Hydrology, 212-213:198-212. DOI:10.1016/S0022-1694(98)00253-4

Bos M.G., Kselik R.A.L, Allen R.G., Molden D. (2009) - Water requirements for irrigation and the environment. Springer Science + Business Media B.V.

Choudhury, B.J., Ahmed, N.U., Idso, S.B., Reginato, R.J., Daughtry, C.S.T., (1994) - Relations between evaporation coefficients and vegetation indices studied by model simulations. Remote Sensing of Environment, 50(1):1-17.DOI:10.1016/0034-4257(94)90090-6

Domingo F., Villagarcy L., Boer M.M., Alados-Arboledas L., Puigdefa´bregas J. (2001) - Evaluating the long-term water balance of arid zone stream bed vegetation using evapotranspiration modeling and hill slope runoff measurements. Journal of Hydrology, 243: 17–30. DOI:10.1016/S0022-1694(00)00398-X

Hemakumara M., Chandrapala L., Moene A.F. (2003) - Evapotranspiration fluxex over mixed vegetation areas measured from large aperture scintillometer. Agricultural water management 88:109-122. DOI:10.1016/S0378-3774(02)00131-2

Farah H., Bastiaanssen W.G.M. and Feddes R.A. (2004) - Evaluation of the temporal variability of the evaporative fraction in a tropical watershed. International Journal of Applied Earth Observation and Geoinformation 5 ,129-140. doi:10.1016/j.jag.2004.01.003

Jia L., Su Z., van den Hurk B., Menenti M., Moene A., De Bruin H.A.R., Yrisarry J.J.B., Ibanez M., Cuesta A., (2003) - Estimation of sensible heat flux using the Surface Energy Balance System (SEBS) and ATSR measurements. Physics and Chemistry of the Earth, Parts A/B/C, 28(1-3): 75-88. DOI:10.1016/S1474-7065(03)00009-3

Jin X., Wan L., Su Z. (2005) - Research on evaporation of Taiyuan basin area by using remote sensing. Hydrology and earth system science discussion. 2:209-227. DOI:10.5194/hessd-2-209-2005

Kerr Y.H., Lagouarde J.P., Imbernon J. (1992). - Accurate land surface temperature retrieval from AVHRR data with use of an improved split window algorithm. Remote Sensing of Environment. 1992. 41(2-3), 97-209. DOI: 10.1016/0034-4257(92)90078-X

Liang S., (2000) - Narrowband to broadband conversions of land surface albedo I: Algorithms. Remote Sensing of Environment 76: 213-238. DOI: 10.1016/S0034-4257(00)00205-4

Loukas A., Vasiliades L., Domenikiotis C., Dalezios N.R. (2005) - Basin-wide actual evapotranspiration estimation using NOAA/AVHRR satellite data. Physics and Chemistry of the Earth 30, 69–79.DOI: 10.1016/j.pce.2004.08.023

Marjanizadeh S. (2008) - Developing a "best case scenario" for Karkheh River Basin management (2025 horizon); a case study from Karkheh River Basin, Iran. Ph.D. thesis, University of Natural Resources and Applied Life Sciences, Vienna

Menenti M. and Choudhury B.J. (1993) - Parametrization of land surface evapotranspiration using a location-dependent potential evapotranspiration and surface temperature range. In: Exchange processes at the land surface for a range of space and time scales, Bolle, H.J. et al. (Eds.). IAHS Publ. no. 212: 561–568.

Muthuwatta L.P, Ahma M.D., Bos M.G., and Rientjes T.H.M. (2010) - Assessment of water availability and consumption in the Karkheh River Basin –Iran- Using remotesensing and geo-statistics. Water resources management 24:459-484. DOI: 10.1007/s11269-009-9455-9

Su Z. and Jacobs C. (Eds.), (2001) - Advanced Earth Observation - Land Surface Climate. Report USP-2, 01-02, Publications of the National Remote Sensing Board (BCRS). 184pp.

Su Z. (2002) - The Surface energy balance system (SEBS) for estimation of turbulent heat flux. Hydrology and Earth System Sciences 6(1): 85-89. DOI:10.5194/hess-6-85-2002

Su Z., Yacob A., Wen J., Roerink G., He Y., Gao B., Boogaard H., Diepen C.V. (2003) - Assessing relative soil moisture with remote sensing data: theory, experimental validation, and application to drought mobitoring over the Nortyh China Plain. Physics and Chemistry of the Earth 28:89-101. DOI:10.1016/S1474-7065(03)00010-X

Tasumi M. (2003) - Prograss in operational estimation of regional evapotranspiration using satellite imagery. Phd thesis. University of Idaho.

Teixeira A.H. de Castro, Bastiaanssen W.G.M., Ahmad M.D., Moura M.S.B., Bos M.G. (2008) - Analysis of energy fluxes and vegetation-atmosphere parameters in irrigated and natural ecosystems of semi-arid Brazil. Journal of Hydrology. 362: 110-127. DOI:10.1016/j.jhydrol.2008.08.011

Valor E., Caselles V. (1996). - Mapping land surface emissivity from NDVI: Application to European, African, and South American areas. Remote Sensing of Environment 57, pp. 167-184. DOI: 10.1016/0034-4257(96)00039-9